

Published in final edited form as:

Nanomedicine. 2015 January ; 11(1): 167–173. doi:10.1016/j.nano.2014.08.012.

Nano-Immunoassay with Improved Performance for Detection of Cancer Biomarkers

Alexey V. Krasnoslobodtsev^{1,5,*}, María P. Torres², Sukhwinder Kaur², Ivan V. Vlassiouk³, Robert J. Lipert⁴, Maneesh Jain², Surinder K. Batra^{2,*}, and Yuri L. Lyubchenko^{1,*}

¹Department of Pharmaceutical Sciences, University of Nebraska Medical Center, Omaha, NE 68198

²Department of Biochemistry and Molecular Biology, University of Nebraska Medical Center, Omaha, NE, 68198

³Oak Ridge National Laboratory, Oak Ridge, TN 37831

⁴Iowa State University, Ames, IA 50011

⁵Department of Physics, University of Nebraska Omaha, Omaha, NE 68182

Abstract

Nano-immunoassay utilizing surface-enhanced Raman scattering (SERS) effect is an analytical technique with high sensitivity that holds a great promise for early cancer detection. In its current standing the assay is capable of discriminating samples of healthy individuals from samples of pancreatic cancer patients. Further improvements in sensitivity and reproducibility will extend practical applications of the SERS-based detection platforms to wider range of problems. In this report, we discuss several strategies designed to improve performance of the SERS-based detection system. We demonstrate that reproducibility of the platform is improved by using atomically smooth mica surface as a template for preparation of capture surface in SERS sandwich immunoassay. Furthermore, assay's stability and sensitivity can be further improved by using either polymer or graphene monolayer as a thin protective layer applied on top of the assay addresses. The protective layer renders signal to be more stable against photo-induced damage and carbonaceous contamination.

Keywords

Nano-immunoassay; cancer biomarkers; nanodiagnostics; pancreatic cancer; surface-enhanced Raman scattering (SERS); AFM

© 2014 Elsevier Inc. All rights reserved.

Send the correspondence to: Alexey V. Krasnoslobodtsev, Ph.D., Department of Physics, University of Nebraska Omaha, 6001 Dodge Street, Omaha, NE 68182-0266, U.S.A., 402-554-3723 (office), 402-554-3100 (fax), akrasnos@gmail.com. *Corresponding authors.

Conflict of Interest: We declare no conflicts of interest.

Publisher's Disclaimer: This is a PDF file of an unedited manuscript that has been accepted for publication. As a service to our customers we are providing this early version of the manuscript. The manuscript will undergo copyediting, typesetting, and review of the resulting proof before it is published in its final citable form. Please note that during the production process errors may be discovered which could affect the content, and all legal disclaimers that apply to the journal pertain.

Background

Detection of cancer at early stages can significantly impact survival of cancer patients as exemplified by progress made in prostate and breast cancer. Surface enhanced Raman scattering (SERS) has emerged as a strong platform for the development of sensitive immunoassays that are capable of detecting low levels of analytes from small sample volumes. High sensitivity and the wealth of chemical information in the readout signal (Raman spectrum) provide a great potential of SERS in detecting low amounts of biomarkers that may be present at the asymptomatic early stages of disease. Additional attractive features of SERS readout methodology include narrow spectral bandwidth and the ability to perform multiplexed analysis of several markers using a single excitation wavelength.^{1, 2} A wide range of applications using SERS for detection of nucleic acids, proteins, and other analytes have been realized in recent years.³⁻⁷ The development of reliable and quantitative SERS based platform for detection of disease biomarkers is a long-term pursuit that would lead to early and accurate diagnosis of many diseases including cancer.

Serum-based assays are the most used tests for the detection of tumor markers in clinical settings. The ability to detect specific cancer biomarkers in human serum provides an effective test for early diagnosis, predicting relapse, prognosis, and assessing response to therapy. Expression of mucins, high molecular weight and heavily glycosylated proteins, has been considered as one of the most prominent characteristics in many types of cancer. It has been demonstrated that the mucin protein, MUC4, is overexpressed in pancreatic cancer.⁸ The expression levels of MUC4 are increased with advancing stages of pancreatic cancer,⁹ suggesting that MUC4 can serve as a potential biomarker in serum-based assay for early diagnosis of this disease.¹⁰ Conventional bioassays routinely used in clinical settings such as enzyme linked immunosorbent assay (ELISA) and radioimmunoassay (RIA) could not detect MUC4 in serum. We have recently developed a MUC4 detection platform based on surface-enhanced Raman scattering (SERS) with a readout surpassing the analytical capabilities of both conventional enzyme-linked immunosorbent assay (ELISA) and radioimmunoassay (RIA) to detect MUC4.¹⁰

In this report, we have utilized the existing potential of the SERS-based assay to detect low levels of cancer biomarkers in human serum. We demonstrated that the assay's superior sensitivity allows for discrimination of serum samples from healthy individuals and pancreatic cancer patients. Further assay optimization, especially for its practical applicability in clinical settings, is related to such key issues as stability and reproducibility of the SERS signal. We made a number of improvements in the assay to circumvent some of the problems of SERS-based methodology.

During optimization of the assay components we experimentally demonstrated that atomically flat mica surface used as a template in template-stripped-gold (TSG) strategy greatly improves reproducibility of the SERS signal. Additional merit was observed by using the recently introduced imaging technique¹¹ that involves mapping and subsequent averaging of the characteristic peaks of Raman reporter molecules. Other problems inherent to SERS include signal loss and contamination of the spectra with a wide peak from

amorphous carbon observed upon strong and/or prolonged illumination of the samples. We introduce modifications to the assay in order to minimize these issues by applying a thin protective layer on top of prepared, ready-to-use samples. The application of this layer results in cleaner and more stable SERS signals thereby improving the stability and reproducibility of the assay. The results of this study can serve as practical guidelines for further optimization and development of highly stable and sensitive SERS immunoassay platform that would enable a direct, reliable and affordable detection of low levels of biomarkers in various systems.

Methods

Reagents and materials

Mica muscovite (Asheville-Schoonmaker Mica Co., Newport News, VA), gold of 99.9 % purity (Kurt J. Lesker Company, Jefferson Hills, PA). Methanol, sodium chloride, dithiobis-(succinimidyl propionate) (DSP), dimethylsulfoxide (DMSO), phosphate buffered saline (PBS) packs (10 mM), bovine serum albumin (BSA), octadecanethiol (ODT), and 4-Nitrobenzenethiol (NBT) all from Sigma (Sigma-Aldrich, St. Louis, MO); polydimethylsiloxane as Sylgard 184 – a two component elastomer kit (Dow Corning Corporation, Midland, MI), the two component epoxy glue EPO-TEK 353ND (Epoxy Technology, Inc., Billerica, MA), and gold colloidal nanoparticles with nominal diameters of 60 nm (Ted Pella, Redding, CA).

Preparation of Extrinsic Raman Labels (ERL)

The detailed procedure for the preparation of ERL has been described in ¹⁰. Briefly, gold nanoparticles (60 nm in diameter) were modified with a mixed thiol solution of DSP (2 μ L of 1 mM solution) and NBT (4 μ L of 2mM solution) where NBT serves as a Raman reporter molecule and DSP links antibody to the nanoparticles via amine reactive N-hydroxysuccinimide ester. The coverage of the MUC4-specific monoclonal antibody 8G7 bound to gold nanoparticles was optimized by using a range of concentrations of antibodies in a solution used for modification of the nanoparticles between 0.1 μ g/mL and 20 μ g/mL to find the optimal coverage. To assess the performance of the ERL's with different antibody concentrations we monitored the intensity of the Raman signal at 1336 cm^{-1} while changing the amount of the cell (CD18/HPAF) lysate (0, 1, 2, 4, 6, 8, 10 μ g/mL). The optimal coverage was achieved at 0.1 μ g/mL of the antibody and this concentration was further used in this study.

Preparation of capture substrates

A substrate template, either silicon or mica, was coated with 250 nm of gold (a resistive evaporator (Edwards Auto 306/silicon)¹⁰ and an ion beam sputter system (IBS/e, South Bay Technology/mica). Next, a glass chip is glued onto the topside of the gold layer using epoxy glue. Fresh gold surface (i.e. Template Stripped Gold - TSG) is created when the glass chip is pulled away separating gold from a template. Gold surface used for sample preparation was thus created at the interface of gold with the template. The capture surface was stamped, coated with ODT and capture antibody as described previously.¹⁰ The capture surface optimization involved testing various concentrations of the anti-MUC4 monoclonal antibody

8G7 and varied between 1 $\mu\text{g}/\text{mL}$ and 100 $\mu\text{g}/\text{mL}$. The optimal coverage as determined from the intensity of the Raman signal at 1336 cm^{-1} was achieved at 5 $\mu\text{g}/\text{mL}$ of the antibody. For experiments with protective layer, a thin layer of polydimethylsiloxane (PDMS) was applied using spin-coating system at 2000 rpm using a Model WS-400BZ-6NPP/LITE spin coater (Laurell Technologies Corporation, North Wales, PA) from a solution containing mixture of PDMS and hexane (v/v 1:20) followed by curing overnight. Graphene was grown by Chemical Vapor Deposition on Cu catalyst (metal sheet) as described in ¹². Graphene monolayer was then applied on top of the addresses using polymethyl methacrylate (PMMA) transfer procedure.¹²

Clinical samples

This retrospective study for serum biomarkers in PC was approved by the Institutional Review Board (IRB) of the University of Nebraska Medical Center (UNMC) (IRB number 209-00). Written informed consent was obtained from PC patients and controls for enrollment into the study. Inclusion criteria for PC patients was any adult subject (age 18 years) with histologically proven PC while healthy controls were age-matched volunteers. Serum samples from 5 PC patients and 5 healthy controls were evaluated for circulating MUC4 level (Table 1). Following collection by a nurse coordinator, the blood samples were allowed to clot for 30 min at room temperature and sample aliquots were stored at -80°C until MUC4 assay. For PC patients, only treatment naïve samples withdrawn prior to any cancer-directed surgical, radiological or chemotherapeutic intervention were used. PC staging was based on one of four criteria: 1) pathological staging post-surgery 2) MRI/CT/ultrasound staging if this was the only staging available, 3) endoscopic staging if the patient never underwent surgery or 4) biopsy of metastatic disease if no previous staging was available.

SERS measurements

Raman spectra were collected with Ntegra Spectra (NT-MDT, Russia) using 632.8 nm He-Ne laser with power at the sample being ~ 0.1 mW. The sample was placed directly under the objective lens (Mitutoyo, 0.9 NA, 100X). SERS spectra were recorded by focusing laser light on the surface at 90 degrees of incident angle. The same objective was used to collect the scattered light. Integration time for each spectrum was 5 sec.

Results

Experimental setup

Figure 1 schematically shows the experimental approach used in this study. The nanoparticle-based SERS platform for detecting cancer biomarkers uses a sandwich format and consists of the following components: 1) gold capture surface (Figure 1, A) and 2) extrinsic Raman labels (ERL – Figure 1, B). Capture surface is prepared on a template stripped gold (TSG) substrate. The surface is modified with specific antibodies using thiolated linker molecules (DSP). ERLs are gold nanoparticles also modified with the same specific antibodies along with Raman reporter molecules (RRM's). A capture surface specifically binds and concentrates analytes from the sample (Figure 1, C). Exposure of this substrate to a solution containing ERLs results in binding of an ERL to the capture surface

via antibody-antigen interaction in a sandwich format (Figure 1, C). Subsequent interrogation of the sample with the laser light produces readout signal, SERS spectrum - a “fingerprint” profile unique to the Raman reporter molecules (Figure 1, D).

To accomplish the goal of this study we used a highly selective monoclonal antibody 8G7¹³ which was immobilized on both gold substrate and gold nanoparticles. The sandwich assay using the same antibody for capture and detection was feasible due to the repetitive nature of the epitope recognized by 8G7. Cell lysate from MUC4-expressing pancreatic cancer cells was utilized as antigen and the gold nanoparticles were decorated with 4-nitrobenzenethiol (NBT). Each nanoparticle carries a large number of RRM's (10^3 – 10^4)¹⁰ contributing to a significantly enhanced signal from individual binding event. Additionally, SERS is generated by gold nanoparticles and further amplified by the close proximity of the gold substrates.^{1, 14} The SERS amplification is a result of strong plasmonic coupling between nanoparticles and the surface. First, plasmon oscillations of the particle, excited by the laser, couple to free electrons in the gold surface producing an enhanced electric field that is scattered by the RRM's. Second, SERS intensity is increased because this coupling shifts the plasmon band of the nanoparticles into resonance with the excitation wavelength of the laser (633 nm).¹⁴ This provides a readout strategy that rivals that of fluorescence giving an advantage of this methodology in comparison with conventional test platforms such as enzyme linked immunosorbent assay (ELISA).¹⁰ High sensitivity of the methodology allows for detection of single ERL nanoparticle.¹

Indeed, our assay produces intense readout signal as SERS spectrum (Figure 1, D). The spectrum has several representative Raman bands which can be easily assigned to the vibrational modes of the Raman reporter molecule - NBT. The most dominant band at $\sim 1336\text{ cm}^{-1}$ belongs to a symmetric stretch of NO_2 group and the intensity of this band depends proportionally on the concentration of MUC4 in a sample. The intensity of this band was used for all the characterizations of the assay performance at concentrations of MUC4 that produce signal intensity well above limit of detection corresponding to signal intensity of a blank sample.

We applied the developed approach to demonstrate its capability to detect MUC4 in serum samples from individual patients. Figure 2 shows a comparative graph of the average values and standard deviations for serum samples of 5 healthy individuals (left side of the graph) and 5 patients with pancreatic cancer (right side of the graph). The graph demonstrates that samples from PC patients produced significantly higher signal intensities than samples from healthy individuals. As mentioned above, conventional methods routinely used in clinical settings, ELISA and RIA, have not been able to detect MUC4 in sera samples indicating superiority of the developed SERS-based assay and its potential in cancer diagnostics.

Assay Reproducibility. Effect of surface topography

Theoretical and experimental studies suggested that the plasmon coupling between gold nanoparticles and the underlying metallic surface is very sensitive to the distance between contacting surfaces.^{1, 15, 16} Since the biggest SERS is generated at the junction between nanoparticles and the surface, the nanoscale characteristics (smoothness) are important contributors to the SERS enhancement. Thus, controllable and reproducible synthesis of the

components is critical for the reproducibility of the assay. One critical component is gold nanoparticles where homogeneity in size is important for the signal amplification.¹⁴ Commercially available nanoparticles have very high degree of homogeneity in terms of particle diameter eliminating the need for further improvement. Another critical component of the assay is gold surface topography and this issue received a thorough study.

Figure 3 shows AFM images of template-stripped gold surfaces using silicon wafer (Figure 3, A) and mica (Figure 3, B) as a template. TSG procedure using silicon as a template produced surface with roughness RMS=7.3 nm. TSG prepared using mica as a template is much smoother with RMS=0.5 nm. Both surfaces were compared using the same preparation procedure and the same concentration of antigen, MUC4, in solution (62.5 µg/mL). The intensity of the Raman signal characteristic of the symmetric nitro stretch (at ~1336 cm⁻¹) for the Raman reporter, 4-nitrobenzenethiol, was collected on 49 various spots on the surface. Figure 3, C shows intensities of the Raman signals detected across a single address for Si-TSG (diamonds) and Mica-TSG (circles). The data demonstrates that signal intensities for Si-TSG exhibit a larger variability compared to that of Mica-TSG. Signals as low as 5096 counts and as high as 51519 counts were detected using Si-TSG, while Mica-TSG produced a much narrower range of values with 6126 and 21825 counts respectively. The comparison of averaged Raman intensities (RI) for the assay is shown on the right panel of Figure 3, C. Averaged intensities are RI=14100 counts for Si-TSG (red cross) and RI=11800 counts for Mica-TSG (green circle). The bars on the graph represent standard deviation (SD) of statistically averaged Raman intensities. Standard deviation for mica-TSG is much smaller, SD=3600, as compared to Si-TSG surface, SD=9800. These results indicate that roughness of the substrate contributes to variation in signal enhancement across the substrate. Therefore, using smoother gold surface provides more reproducible signal intensity detected across the sample.

Response of the assay to prolonged illumination

SERS platform for analytical purposes requires the illumination of samples with intense laser light. We examined stability of our assay by measuring the dependence of the Raman signal intensity at 1336 cm⁻¹ on duration of sample exposure to laser light. Figure 4, A (diamonds) indicates that the intensity of the signal decreases with time. A fast decrease is observed within first few minutes leveling off at longer exposure times. The intensity of the Raman signal does not drop to zero even after long period of illumination. As Figure 4, A shows the signal reaches 17 % of the initial intensity at 15 min of total illumination time.

Not only did the intensity of the characteristic bands decline upon prolonged illumination of the sample, the recorded spectrum itself changes with time. Figure 4, B shows several representative spectra with time evolution of the spectrum. Although, initially there is only reduction of the signal intensity, the contamination of the spectra with a wide peak ranging from ~1000 cm⁻¹ to ~1700 cm⁻¹ is observed at longer exposure times (Figure 4, B). Such spectra contamination is usually related to the accumulation of amorphous carbon.¹¹ Indeed two maxima of the broad peak corresponding to D-band of carbon at ~1360 cm⁻¹ and G-band at ~1580 cm⁻¹ can be distinguished in some spectra. The origins of this contamination are not fully understood, however such factors as photo-induced or thermal decomposition

of the analyte molecules are usually discussed in the literature.¹⁷ Another possible source of carbon contamination is adsorption of airborne hydrocarbons on the metal surface.¹⁸ Other components of our assay such as antibodies and proteins may all contribute to the appearance of the carbonaceous peaks upon their decomposition.

Both signal deterioration and accumulation of broad peaks from carbonaceous contamination are considered to be ubiquitous problems of SERS methodology. The presence of these problems limits quantitative analysis of readout signal in sensor applications and prevents the development of reliable and quantitative SERS based detection platform. Next section discusses our solution to these limitations.

Effect of the overcoat on the assay performance

As we indicated above, a prolonged exposure to intense laser light leads to photo-induced and thermal decomposition of the RRM's as well as contamination of the observed spectrum with broad bands originating from carbonaceous species. In order to improve stability of the assay and increase the resistance of the RRM's to photo damage we have applied a transparent protective coat of PDMS on top of the SERS addresses. Figure 4, C shows several representative spectra measured at the same time points as for non-coated assay shown in Figure 4, B. The results demonstrate that overcoating of the assay addresses with a thin layer of PDMS improves performance of the assay and helps prevent the appearance of carbonaceous peaks. As with the non-coated assay, the dependence of the signal intensity on exposure time still shows decline of the Raman signal intensity (Figure 4, A: stars). The decline of the signal is much slower than that observed for non-coated assay. Additionally, the signal reaches 38 % of the initial intensity at 15 min which is much higher than for non-coated assay. Although the coating does not completely eliminate degradation of RRM's, it significantly improves the assay performance in terms of signal stability.

We have also used single layer graphene as a protective layer in SERS based analytical assay. A polymer coat was replaced with CVD grown graphene placed atop of the assay. The graphene monolayer is highly transparent (97.3 %) which makes it suitable as protection for our experimental design where excitation and signal collection are achieved in top-illumination configuration (see Figure 1, C). Figure 4, A clearly demonstrates that graphene coated assay (circles) outperforms both normal (non-coated) and PDMS coated assays in terms of signal stability. The signal intensity only slightly changes within first few minutes of the observation. It also shows that the signal at 15 min reaches 60 % of the initial intensity. This level is 3.5 times greater than for non-coated assay and almost 1.6 times greater than for the assay coated with polymer. Additionally, measured spectra are of high quality and much cleaner with lower background (Figure 4, D) which is beneficial for quantitative calculations.

Discussion

The primary focus of this study was to further improve the performance of the nanoparticle-based SERS immunoassay for early detection of cancer biomarkers. Specifically, improvements in reproducibility have been achieved by using mica surface as a template for TSG substrate preparation coupled with imaging mode of SERS. Atomically flat mica

surface was used as a substrate for the gold layer fabrication. The use of mica also reduces contribution of the surface roughness to the SERS signal variation. This finding highlights the importance of reproducible smooth substrate for its application in SERS-based immunoassay.

We also demonstrate that the application of an overcoat atop assay addresses improves performance of the SERS based MUC4 immunoassay indicating the importance of protection for the SERS-based readout. The protective strategy with coating applied on top of the assay improves signal stability compare to uncoated assay. Also, unlike other protective strategies, for example silica shell on Au nanoparticles, our strategy allows for additional plasmonic coupling between Au surface and Au nanoparticles enhancing thus the measured signal. The application of a protective layer on top of the SERS assay not only leads to a higher stability of the signal but also prevents uncontrolled sample carbonization. With elimination of these factors it becomes possible to improve sensitivity of the assay by increasing time of signal acquisition. Both coating materials, polymer and graphene, performed better than bare non-coated assay. One possible explanation of the improved signal stability is that the coating provides a shield for the RRM's against photodecomposition and prevents adsorption of contaminants from the atmosphere onto active plasmonic nanoparticles. Another alternative explanation to the improved performance of the assay is that the coating reduces the effect of local heating by the tightly focused laser beam. It is also possible that gold nanoparticles absorb light and effectively convert it into heat as has been previously reported.¹⁹ Thus, local temperature can be dramatically increased by laser irradiation. Such local heating can distort Raman spectra due to gradual thermal decomposition of Raman reporters. Desorption of Raman reporters from nanoparticles at elevated temperatures can also cause signal degradation. Indeed, air is the poorest heat conductor with thermal conductivity, κ_{air} , being 0.024 W/m K. Thermal conductivity of PDMS is higher, $\kappa_{\text{PDMS}} = 0.15$ W/m K, allowing for better heat dissipation and, thus, better performance of the Raman reporter molecules. Graphene with its thermal conductivity estimated to be in the range of ~ 5000 W/m K is the best heat conductor.^{12, 20} The increase in stability follows the same trend as thermal conductivity supporting our conclusion that effective heat dissipation at least in part contributes to the enhanced stability of RRM's. While both materials improved performance of the assay, coating with graphene monolayer showed greater benefit for signal stability. Graphene monolayer is only one atom thick but possesses high mechanical strength²¹ and impermeability to gases.²² These advantageous properties of graphene along with its high thermal conductivity can be exploited for constructing SERS based nanosensors with advanced stability and improved sensitivity.

Coating of the prepared assays also contributes to long-term stability of the samples where all the components of the assay are sealed with either polymer or graphene. The seal reduces the influence of environmental conditions (humidity, temperature, oxygen) and prevents deterioration of the components upon prolonged storage. Thus, our findings can be considered as practical guidelines for constructing analytical devices based on SERS readout. Further assay optimization will identify effective ways to improve protection and convenience of assay preparation suitable for Point of Care and in vitro diagnostics. The developed nano-immunoassay in its current standing has superior performance as compared

with conventional methods routinely used in clinical settings. The assay is capable of detecting and quantifying levels of MUC4 in individual serum samples. It also distinguishes samples of PC patients from healthy individuals indicating the potential of the developed SERS-based assay in cancer diagnostics.

Acknowledgments

We thank Yuliang Zhang for help in automation of data analysis.

Financial support: The work was supported by grants EPS – 1004094 (NSF) and 5R01GM096039-04 (NIH) to YLL; National Institutes of Health (EDRN UO1 CA111294, P50 CA 127297) to SKB and Nebraska Research Initiative (NRI) grant to MJ, YLL and AVK.

References

1. Porter MD, Lipert RJ, Siperko LM, Wang G, Narayanan R. SERS as a bioassay platform: fundamentals, design, and applications. *Chem Soc Rev.* 2008; 37:1001–11. [PubMed: 18443685]
2. Vo-Dinh T, Wang HN, Scaffidi J. Plasmonic nanoprobe for SERS biosensing and bioimaging. *J Biophotonics.* 2010; 3:89–102. [PubMed: 19517422]
3. Barhoumi A, Zhang D, Tam F, Halas NJ. Surface-Enhanced Raman Spectroscopy of DNA. *J Am Chem Soc.* 2008; 130:5523–5529. [PubMed: 18373341]
4. Wei F, Zhang D, Halas NJ, Hartgerink JD. Aromatic Amino Acids Providing Characteristic Motifs in the Raman and SERS Spectroscopy of Peptides. *The Journal of Physical Chemistry B.* 2008; 112:9158–9164. [PubMed: 18610961]
5. Shafer-Peltier KE, Haynes CL, Glucksberg MR, Van Duyne RP. Toward a Glucose Biosensor Based on Surface-Enhanced Raman Scattering. *J Am Chem Soc.* 2002; 125:588–593. [PubMed: 12517176]
6. Levin CS, Kundu J, Janesko BG, Scuseria GE, Raphael RM, Halas NJ. Interactions of Ibuprofen with Hybrid Lipid Bilayers Probed by Complementary Surface-Enhanced Vibrational Spectroscopies. *The Journal of Physical Chemistry B.* 2008; 112:14168–14175. [PubMed: 18942873]
7. Vitol EA, Brailoiu E, Orynbayeva Z, Dun NJ, Friedman G, Gogotsi Y. Surface-Enhanced Raman Spectroscopy as a Tool for Detecting Ca²⁺ Mobilizing Second Messengers in Cell Extracts. *Anal Chem.* 2010; 82:6770–6774. [PubMed: 20704365]
8. Andrianifahanana M, Moniaux N, Schmied BM, Ringel J, Friess H, Hollingsworth MA, et al. Mucin (MUC) gene expression in human pancreatic adenocarcinoma and chronic pancreatitis: a potential role of MUC4 as a tumor marker of diagnostic significance. *Clin Cancer Res.* 2001; 7:4033–40. [PubMed: 11751498]
9. Chakraborty S, Jain M, Sasson AR, Batra SK. MUC4 as a diagnostic marker in cancer. *Expert Opin Med Diagn.* 2008; 2:891–910. [PubMed: 23495864]
10. Wang G, Lipert RJ, Jain M, Kaur S, Chakraborty S, Torres MP, et al. Detection of the potential pancreatic cancer marker MUC4 in serum using surface-enhanced Raman scattering. *Anal Chem.* 2011; 83:2554–61. [PubMed: 21391573]
11. Yeo BS, Schmid T, Zhang W, Zenobi R. A strategy to prevent signal losses, analyte decomposition, and fluctuating carbon contamination bands in surface-enhanced Raman spectroscopy. *Appl Spectrosc.* 2008; 62:708–13. [PubMed: 18559160]
12. Vlassiouk I, Smirnov S, Ivanov I, Fulvio PF, Dai S, Meyer H, et al. Electrical and thermal conductivity of low temperature CVD graphene: the effect of disorder. *Nanotechnology.* 2011; 22:275716. [PubMed: 21613685]
13. Moniaux N, Varshney GC, Chauhan SC, Copin MC, Jain M, Wittel UA, et al. Generation and Characterization of Anti-MUC4 Monoclonal Antibodies Reactive with Normal and Cancer Cells in Humans. *Journal of Histochemistry & Cytochemistry.* 2004; 52:253–261. [PubMed: 14729877]

14. Driskell JD, Lipert RJ, Porter MD. Labeled gold nanoparticles immobilized at smooth metallic substrates: systematic investigation of surface plasmon resonance and surface-enhanced Raman scattering. *J Phys Chem B*. 2006; 110:17444–51. [PubMed: 16942083]
15. Okamoto T, Yamaguchi I. Optical Absorption Study of the Surface Plasmon Resonance in Gold Nanoparticles Immobilized onto a Gold Substrate by Self-Assembly Technique. *The Journal of Physical Chemistry B*. 2003; 107:10321–10324.
16. Hutter T, Huang FM, Elliott SR, Mahajan S. Near-Field Plasmonics of an Individual Dielectric Nanoparticle above a Metallic Substrate. *The Journal of Physical Chemistry C*. 2013; 117:7784–7790.
17. Khan I, Polwart E, McComb DW, Smith WE. Correlation of optical properties with structure of immobilised nanoparticles--a method for probing the mechanism of SERRS. *Analyst*. 2004; 129:950–5. [PubMed: 15457329]
18. Otto A. What is observed in single molecule SERS, and why? *Journal of Raman Spectroscopy*. 2002; 33:593–598.
19. Fedoruk M, Meixner M, Carretero-Palacios S, Lohmuller T, Feldmann J. Nanolithography by Plasmonic Heating and Optical Manipulation of Gold Nanoparticles. *ACS Nano*. 2013
20. Balandin AA, Ghosh S, Bao W, Calizo I, Teweldebrhan D, Miao F, et al. Superior thermal conductivity of single-layer graphene. *Nano Lett*. 2008; 8:902–7. [PubMed: 18284217]
21. Lee C, Wei X, Kysar JW, Hone J. Measurement of the elastic properties and intrinsic strength of monolayer graphene. *Science*. 2008; 321:385–8. [PubMed: 18635798]
22. Bunch JS, Verbridge SS, Alden JS, van der Zande AM, Parpia JM, Craighead HG, et al. Impermeable Atomic Membranes from Graphene Sheets. *Nano Lett*. 2008; 8:2458–2462. [PubMed: 18630972]

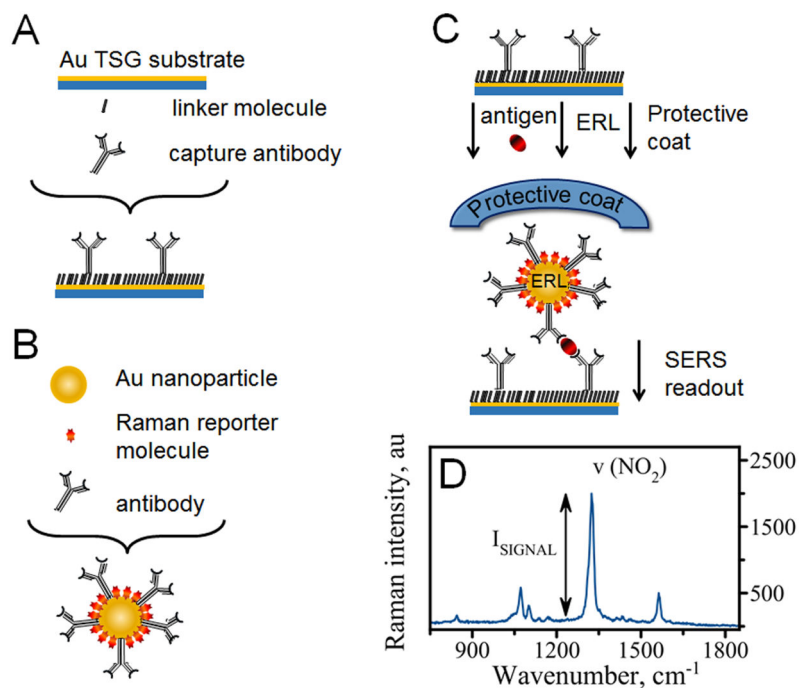


Figure 1.

Scheme showing the design of the SERS-based nano-immunoassay: (A) a gold capture substrate modified with linker molecules and antibodies; (B) gold nanoparticles (ERLs) functionalized with Raman reporter molecules (RRM's) and specific antibodies; (C) sandwich immunoassay where antibodies on the capture surface first bind antigen and subsequently bind ERL; (D) The sandwiched assay produces SERS readout with several characteristic bands from NBT Raman reporter molecule. The most prominent is $\nu(\text{NO}_2)$ - a symmetric nitro stretch at 1336 cm^{-1} .

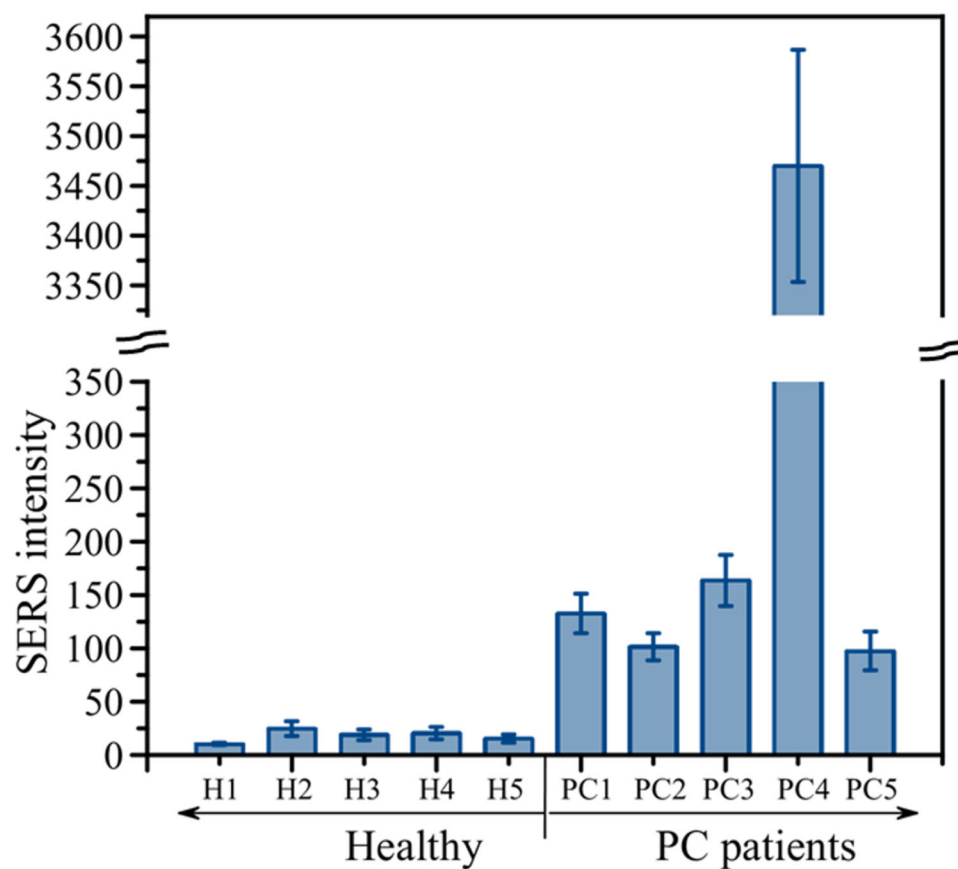


Figure 2. A comparative graph of the average values and standard deviations for serum samples of 5 healthy individuals (left side of the graph) and 5 patients with pancreatic cancer (right side of the graph). Demographic information of each individual sample is provided in Table 1.

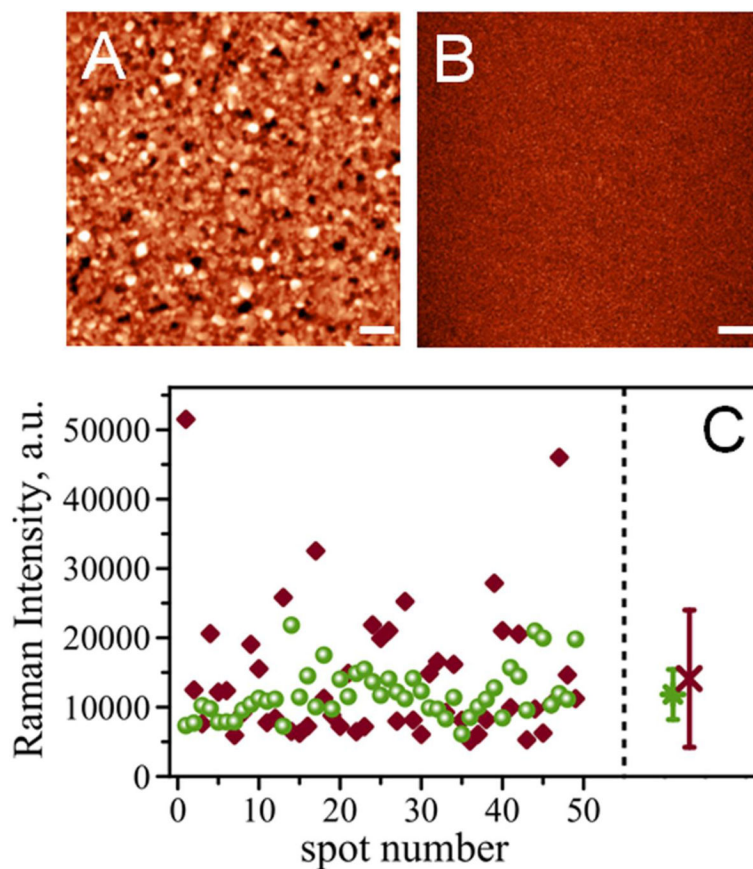
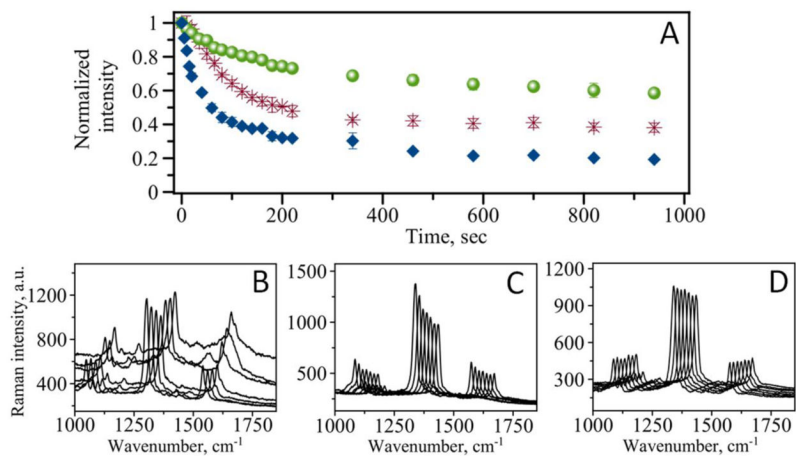


Figure 3. AFM topography of template-stripped gold surfaces using (A) silicon wafer as a template and (B) mica as template with the same z-scale. Scale bar is 1 μm. (C) comparison of Raman intensities for gold surfaces stripped from silicon wafer (diamonds) and mica based (circles) measured as a map of 7 by 7 spectra on a 50 μm area. Right panel: averaged RI for silicon (at 14100 counts, red cross) and mica (at 11800 counts, green circle); corresponding standard deviation values are shown as error bars.

**Figure 4.**

(A) Time dependence of Raman signal intensity for non-coated (blue diamonds), PDMS coated (red stars), and graphene coated (green circles) MUC4 immunoassay. (B) Representative spectra for non-coated assay taken at 20 sec interval. (C) Representative spectra for PDMS coated assay taken at 20 sec interval. (D) Representative spectra for graphene coated assay taken at 20 sec interval.

Table 1

Demographic information on patients used in the study.

Serum sample	Diagnosis	Sex	Age	Race	PRE or post- surgical specimen	Stage (TNM)	Grade of Differentiation	History of Smoking
PC1	PDAC	FEMALE	61	White	PRE	2b	Poor	Y
PC2	PDAC	MALE	58	White	PRE	4	N/A	N
PC3	PDAC	MALE	62	White	PRE	4	N/A	Y
PC4	PDAC	MALE	79	White	PRE	4	Moderate	Y
PC5	PDAC	MALE	75	White	PRE	4	Poor	Y
H1	Control	MALE	60	White	-	-	-	N/A
H2	Control	FEMALE	52	White	-	-	-	N/A
H3	Control	FEMALE	58	White	-	-	-	N/A
H4	Control	FEMALE	62	White	-	-	-	N/A
H5	Control	FEMALE	66	White	-	-	-	N/A